Cold rolling techniques in mechanical splices: Experimental investigations

Mohamad Reza Shokrzadeh[1,3*], Taleb Sadeghian[2], F. Nateghi-Alahi[3]

[1] Department of Civil Engineering, Science and Research Branch, Islamic Azad University, Tehran, Iran

[2] Department of Earthquake Engineering, Shahid Ashrafi Esfahani University, Esfahan, Iran

[3]International Institute of Earthquake Engineering and Seismology, Tehran, Iran

ABSTRACT

This study presents a comprehensive evaluation of the performance of oversize threaded splices under cyclic loading conditions. The research includes monotonic tensile testing and cyclic loading experiments to investigate the seismic behavior of the splices. The experimental results demonstrate that the splices exhibit lower values of εu (strain at peak load) in cyclic loading compared to monotonic tensile testing. This suggests that the cyclic response can serve as a conservative lower bound for the mechanical performance of the splices. The findings highlight the importance of considering cyclic loading conditions when determining conservative lower bounds for the design and evaluation of threaded splices. Understanding the behavior and performance of threaded splices under cyclic loading is crucial for ensuring their reliable and safe operation in seismic regions.

Keywords: Mechanical threaded splice, Ductile Members, Cold rolling, Modifying threaded

1. Introduction

Due to bar length limits, splicing of reinforcing bars is unavoidable in reinforced concrete (RC) structures and may alter the overall behavior of structures under static and dynamic stresses [1,2]. Splicing methods introduced and explored thus far can be divided into three categories: lap, welded, and mechanical splices, each with advantages and disadvantages [3–5]. Lap splicing is the traditional way of splicing that involves arranging a suitable length of connecting bars side by side and can be characterized as contact or non-contact [1,3]. The increased length of the steel bars may produce congestion and may increase the cost due to the higher steel amount. When they are placed in locations with inelastic deformations, it also reduces their strength or displacement capacity [1,6,7]. More importantly, the performance of the lap splice is strongly dependent on the concrete strength. This means that even if the lap splice is correctly constructed and operated, it may fail due to low-strength concrete [2]. Gas pressure welding (GPW) is another splicing technology that was introduced in the 1930s in the United States and Japan [8,9].Rails, steel pipes, and reinforcing bars can all be joined using this technique, which is also known as the forging method. By heating the bars using acetylene and oxygen gases, bars can be joined together using this technique. When they are close to the plastic range, pressure is applied to crimp them together head-to-head [10–12]. The main benefits of this approach are that it can be applied to medium- to large-diameter bars, that it produces splices with acceptable behavior, and that it is quick and affordable. It should be remembered that the effectiveness of this approach depends greatly on the operator's skills; therefore, the price and time required to operate this splice may be comparable to those of a mechanical splice [1]. In the mechanical splice method, couplers are rigid components that are used to join reinforcement bars together. Couplers can be broadly divided into five kinds based on how much stress is transferred between the bars and the couplers: shear screw couplers, headed bar couplers, threaded couplers, grouted couplers, and swaged couplers [2]. Tensile stress in a mechanically spliced bar is transferred from one bar to the other through the coupler and its parts [12,13]. Fast installation, ecologically friendly application, and acceptable performance are all advantages of using mechanical methods [2,14–16]. Bar couplers are categorized as Type 1 or Type 2 by ACI 318 [17]. The strength that a coupler can create serves as the basis for this classification. For instance, a Type 1 coupler is one that can withstand more than 1.25 times the splicing bar's yield strength. According to their strain capacity, "Service" and "Ultimate" couplers are categorized by Caltrans SDC [18]. Couplers can only be used if they can develop a minimum strength of 1.25 times the yield strength of the bar, according to AASHTO [19]. According to the EC8 [20], the use of mechanical couplers for splicing reinforcing bar in the inelastic deformation zones brought on by earthquakes must be tested to ensure that the conditions are consistent with the ductility class that is selected (i.e. medium ductility: DCM, or high ductility: DCH). Current bridge and building design rules forbid the use of mechanical bar splices in the plastic hinge regions of ductile elements in high seismic zones, even though couplers are typically permitted [18,19,21]. Studies done on the performance of mechanical splices can be broken down into three categories: (a) application (with and without concrete), (b) applied load (cyclic or monotonic), and (c) loading rate. All of these studies have come to the same conclusion: splicing all the bars in one area may lead to poor behavior under cyclic load. Steel bars that have been mechanically spliced may fail in the coupler or in the bond between the coupler and the bar [3]. The first kind of failure might have been influenced by the fragile material of the couplers. In this instance, the couplers crack and fail when the spliced bars are subjected to monotonic or cyclic loads. The second type of failure occurs when the bars or sleeves are not properly prepared. Bond failure may be caused by parameters such as thread depth and length in both bars and sleeves (in threaded couplers), insufficient pressure and bar-sleeve lock (in swaged couplers), and incorrect screws in shear screw couplers [1,2,14,15,22–26]. The authors of the studies believe that the most effective parameters for grouted splices are embedded length and sleeve geometry (diameter, length, and thread). An embedded length of 6 d_b and a sleeve length of 16 d_b might produce acceptable performance by increasing the bond capacity [3]. The paper is organized as follows: By modifying the method of making a mechanical bar splice, one type of patch can be introduced that can be used in the plastic hinge areas of ductile members in seismic areas. The splice area in the suggested method is oversized. To enlarge the splice area, one technique—cold rolling—is used. This study conducts uniaxial tensile and cyclic with and without concrete testing on threaded couplers (TC) and oversize-threaded couplers (OTC) reinforcement bar diameters of 16 mm and 20 mm, as well as non-spliced (NS) reference specimens. Strength, ductility, energy absorption, and failure mode performance were evaluated. A thorough explanation of the seismic criteria for the bar splices based on various design standards is also provided in this article for practical use.

2. Experimental program

The behavior of threaded couplers was investigated using uniaxial and cyclic loading. Monotonic static tensile, tension, and compression tests in without concrete were carried out on threaded couplers that join steel bars with different configurations. The tests were performed in the Structures Laboratory at the University of IIEES (the International Institute of Earthquake Engineering and Seismology in Tehran, Iran). Using the Instron Universal Testing Machine (UTM) with a maximum capacity of 600 kN in the static state and a maximum of 500 kN in the dynamic state. The objective was to evaluate the tensile and cyclic behavior of the spliced bars, identify their cause of failure, modify the method of making a mechanical bar splice and combine it with rotary friction welding (two types of patches are introduced that can be used in the plastic hinge areas of ductile members in seismic areas), and use an analytical model to predict the ultimate tensile strength of the threaded splices while taking threaded couplers into consideration. These models are useful for designing RC columns with plastic hinge regions that employ threaded couplers.

2.1. Specimen details

A total of 36 specimens were prepared for the tensile loads and cyclic loads, considering the practical requirements of the plastic hinge areas of ductile members in seismic areas. Two types of tension-compression couplers, namely threaded couplers (TC) and oversize-threaded couplers (OTC), as well as non-spliced (NS) reference specimens, were selected for detailed assessment (as illustrated in **Fig. 1**) with diameters of 16 mm and 20 mm, respectively. Details of the specimen are shown in **Fig. 1** and **Table 1**. To obtain a detailed insight into the with and without concrete response of mechanical splices, uniaxial monotonic and cyclic tests were carried out **(Table 2)**. Specimen ID is broken down into three parts. The first part refers to the specimen that represents the non-spliced (NS), threaded couplers (TC), and oversize-threaded couplers (OTC). The last part identifies the bar size as well as the test protocol (monotonic (tensile test, M) or cyclic (alternating tension and compression test for large plastic strains in mechanical splice, C1, or alternating tension and compression test for high stresses in mechanical splice, C2) **(Table 2)**.

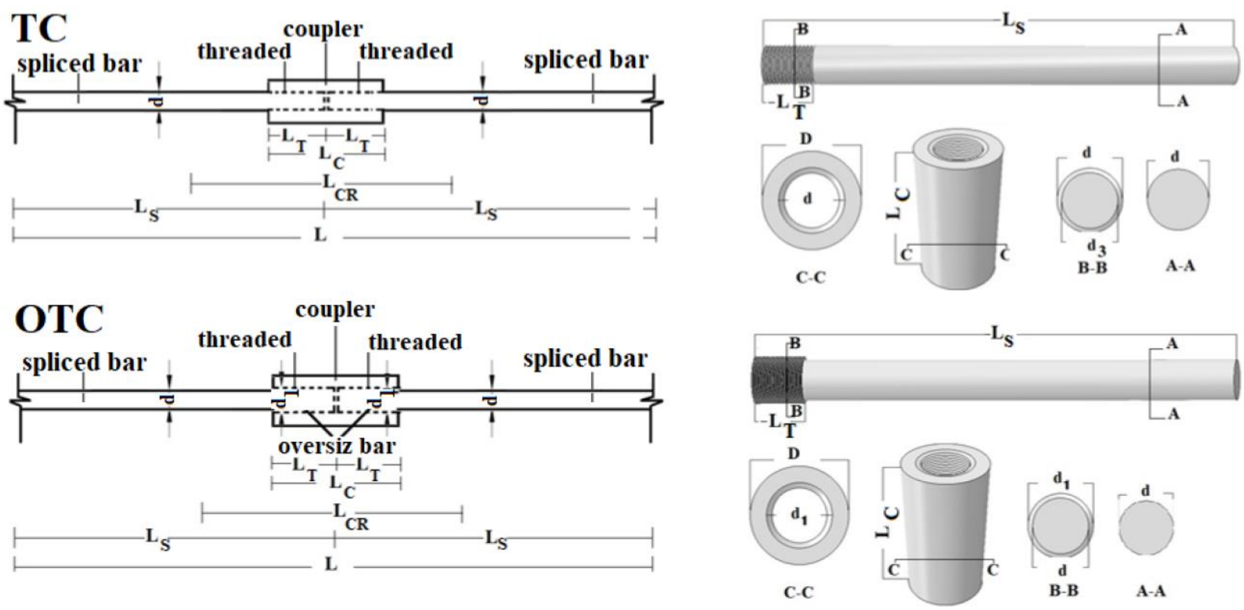

Fig. 1. Details of threaded coupler specimens for TC, OTC, and RFWTC.

Specimen	d_b (mm)	L (mm)	L_S (mm)	L_C (mm)	L_T (mm)	L_W (mm)	L_{Con} (mm)	d_1 (mm)	d_2 (mm)	d_3 (mm)
Non-spliced (NS)	16	700	-	-	-	-	600	-	-	-
	20	700	-	-	-		600	-	-	-
Threaded couplers (TC)	16	700	350	42	21	-	600	16	-	2.5
	20	700	350	50	25	-	600	20	-	2.5
Oversize-threaded coupler (OTC)	16	700	350	46	23	-	600	18	18	2.5
	20	700	360	54	27	-	600	22	22	2.5

Table. 1. Details of test specimens.

	Without concrete tests	
Sample	**Specimen ID**	**Test protocol**
Non-spliced (NS)	A-NS-16M	Monotonic
	A-NS-16C_1	Cyclic C_1
	A-NS-20M	Monotonic
	A-NS-20C_1	Cyclic C_1
Threaded couplers (TC)	A-TC-16M	Monotonic
	A-TC-16C_1	Cyclic C_1
	A-TC-20M	Monotonic
	A-TC-20C_1	Cyclic C_1
Oversize-threaded coupler (OTC)	A-OTC-16M	Monotonic
	A-OTC-16C1	Cyclic C_1
	A-OTC-20M	Monotonic
	A-OTC-20C_1	Cyclic C_1

Table. 2. Monotonic and cyclic test matrix for threaded splice bar specimens.

2.2. Construction and materials

In the TC method, threads are cut into the rebar on both sides. Half of the coupler's length will be the depth of these threads. The assembly is then finished by rotating the rebar (**Figs. 2.a and 2.b**). A special cold rolling method was used to fabricate the OTC specimens; the machine first applied hydraulic pressure to the rebar. The new, bigger thread area allows for a one-size increase in threading size for each rebar. For instance, a 20-rebar after oversizing will have a 22-thread (**Figs. 2.b**). The specimens exposed to monotonic loading had a distance of 700 mm between the testing machine jaws.

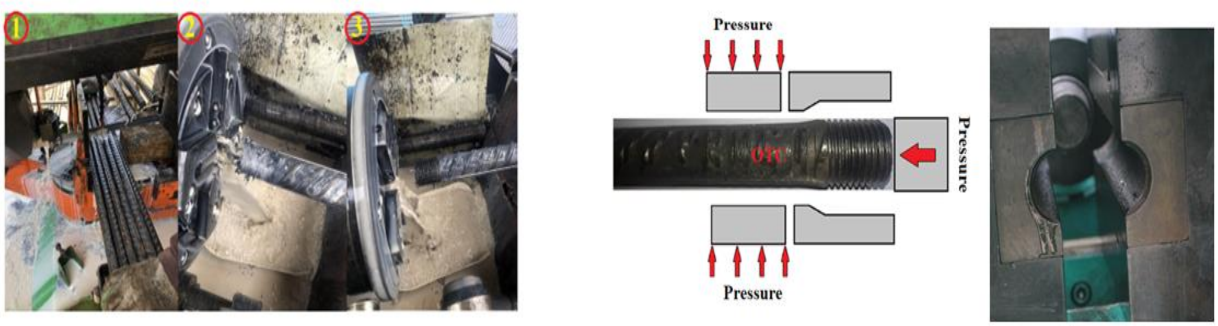

(a) **(b)**

Fig. 2. Construction process of specimens TC and OTC (a) TC, (b) OTC specimens.

2.3. Instrumentation and testing procedures

A static universal testing machine, its hydraulic system, controller, and a test specimen with an extensometer for specimens are shown in **Fig. 3** as the test setup for mechanical bar splices. A sample's maximum length of 1092 mm might be accommodated by the all-purpose testing device. The machine had a 178-mm overall stroke. The machine could produce a force of up to 500 kN in the dynamic state and 600 kN in the static state. Furthermore, the accuracy of the loads and head displacements provided by this universal testing equipment is 1.0 N and 0.0001 mm, respectively. The sampling frequency for machine data was 10 Hz. For all test specimens, a consistent geometry was required to reduce variability in the outcomes. **Fig. 4** displays the chosen geometry for reference non-spliced bars (per ASTM E8 [27]) and spliced specimens, which were created in accordance with the specifications outlined in [28]. Based on the dimensions of the bar and the length of the mechanical bar splice (L_s), the total specimen length (L) was calculated. The coupler length plus α times the bar diameter (α_{db}) from each side of the coupler ends is known as the coupler region length (L_{cr}). In the present study, alpha was more than twice the bar diameter [28]. The bar length from outside the coupler region to the grip was at least 16 times the bar diameter to avoid any localized failure. For regular bar testing, ASTM E8 and ISO ISO/DIS 15835 [27,28] require at least 5 d_b grip-to-grip length. Extensometers were used to measure the strains of non-spliced and spliced specimens, respectively. The bar extensometer had 100-mm stroke and could measure strains until the fracture of the bar. In the monotonic testing of the without concrete mechanical splices, three cycles between zero and 60% yield strength of the non-spliced counterpart were used to evaluate elastic slip at the threads. The identical specimens were then exposed to an axial displacement that increased monotonically until fractur. For without concrete specimens, the yield displacement Δ_y was derived from the test data and utilized to define the key parameters for the cyclic loading technique after getting the whole stress-displacement σ-Δ curve from the monotonic test. The C_1 low-cycle reverse elastic-plastic loading pattern, as specified by ISO 15835-2:2009 [28] and schematically shown in **Fig. 4**, was applied to the cyclic without concrete tests. The loading process involves applying displacements ranging from zero up to 2×Δy (yield displacement) in tension, followed by a reversal corresponding to fifty percent of the yield strength in compression, and repeating this process four times. The applied force is then raised from zero to five times in tension, reversed to 50% of the yield strength in compression, and repeated four times. Following the cycling, the test specimen is subjected to a technique that entails applying increasing tension until failure.

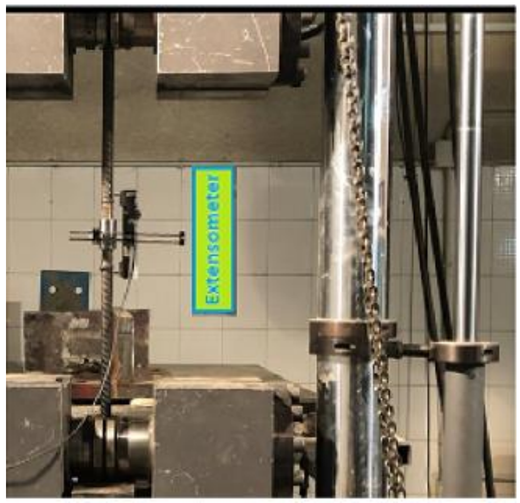

Fig. 3. Testing configuration specimens

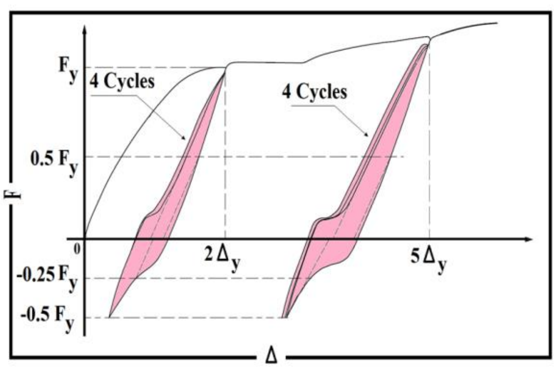

Fig. 4. An illustration of the loading methods in schematic form: C_1 Alternating tension and compression tests for mechanical splices with substantial plastic strains [28].

3. Results and Discussion

3.1. specimens

In this section, monotonic loading and cyclic C_1 loading were used to evaluate 24 mechanical bar splices and 12 non-spliced bars made up of 16 mm and 20 mm splices. These bar sizes were specifically selected since they are available in markets using either SI or Imperial units. Two different types of couplers (TC and OTC) consisting of three different products were included in this experimental program. Two spliced specimens were tested per product, and at least one non-spliced bar was tested per product as the reference sample. The non-spliced samples' minimum tensile yield strength f_y was 511 MPa for 16 mm and 510 MPa for 20 mm, respectively, while their ultimate strength f_u was 618 MPa and 654 MPa, respectively. Both f_y and f_u were calculated by dividing the recorded load by the nominal bar area. The minimal ultimate mean strain u, calculated by dividing the measured displacement by the clear length of the specimen, was ε_u = 0.090 for 16 mm bars and ε_u = 0.090 for 20 mm bars. **Table 3** shows the test findings in terms of yield force F_y and strength f_y, ultimate force Fu and strength fu, mean strain at yield y and ultimate mean strains u, and a ductility factor calculated as the ratio of ultimate-to-yield mean strains $\varepsilon_u/\varepsilon_y$. The stress-strain response of the monotonic and cyclic tests on non-spliced and connected rebars is depicted in **Fig. 5**. All responses, as can be seen from these curves, are within comparable ranges, with ε_u between 0.09 and 0.130, and ε_y being almost identical for each set of tests (16 mm and 20 mm). The slight discrepancies at the end may be related to regular material fluctuations that are inherent. Notably, OTC and OTC coupling systems function effectively under monotonic and cyclic loading. Between the examined configurations, ε_u consistently decreases, as seen by the cyclic loading tests (C_1) in **Fig. 5**. The highest ε_u values were found in the NS and OTC, in the range of 0.13. TC has the greatest reduction in ductility, with an ε_u of 0.09. The production method of mechanical splices with compact couplers has increased the cross-section of the rebar at the threads, which has a positive effect on the strain distribution over the length of the splice with minimal stresses at the coupler region. Some strain localization occurs at the threads in the elastic slip response depicted, as well as at the coupler to rebar interface in the inelastic regime, which ultimately promoted a failure at the coupler region for TC couplers. The ε_u reductions indicated above occur at the splice level and may not characterize the coupler response. Because the coupler has a larger cross-section than the rebar, the weaker segment is transmitted outside of the coupler. As a result, increased strain is created at the rebar, particularly when employing TC couplers, resulting in shorter rebar regions and premature failure near the coupler-to-rebar interface (**Fig. 6**). The decrease in ε_u between splices may become proportionally less important as total specimen length increases. This must also be carefully examined for bending elements with relatively large couplers, as the moment gradient and probable concentration of plasticity in dissipative zones may contribute to ductility reduction [1–3,15].

Specimen	**F_y (kN)**	**F_u (kN)**	**f_y (MPa)**	**f_u (MPa)**	**ε_y (mm/mm)**	**ε_u (mm/mm)**	**μ_ε (ε_{usp}/ ε_{ub})**	**μ (ε_u/ ε_y)**	**R_u (%)**	**Ry (%)**
A-NS-16M-1	102	122	510	623	0.0041	0.122				
A-NS-16M-2	106	127	530	647	0.0038	0.116				
A-NS-16M-3	105	125	525	638	0.0042	0.126				
Average	104±1.7^{ab}	126±2.1^{a}	520±8.5^{a}	636±9.9^{a}	0.0040±0.00017^{a}	0.122±0.004^{a}	1.00	30.40	-	-
A-TC-16M-1	102	121	530	618	0.0041	0.100				
A-TC-16M-2	100	116	525	592	0.0038	0.096				
A-TC-16M-3	106	128	535	653	0.0042	0.102				
Average	103±2.5^{a}	122±4.9^{a}	530±4.1^{a}	622±25^{a}	0.0040±0.00017^{a}	0.098±0.003^{a}	0.80	24.50	119.60	101.53
A-OTC-16M-1	105	125	509	643	0.0040	0.103				
A-OTC-16M-2	109	128	530	653	0.0038	0.101				
A-OTC-16M-3	108	126	520	637	0.0038	0.108				
Average	107±1.7^{ab}	127±1.2^{a}	519±8.6^{a}	644±6.6^{a}	0.0039±0.00017^{a}	0.111±0.003^{a}	0.91	28.46	125.57	99.81
A-NS-16C_1-1	103	123	515	629	0.0044	0.130				
A-NS-16C_1-2	104	124	535	630	0.0044	0.131				
A-NS-16C_1-3	104	123	520	627	0.0043	0.134				
Average	104±0.5^{df}	123±0.5^{de}	524±8.5^{d}	628±1.3^{de}	0.0044±0.00005^{de}	0.132±0.002^{de}	1.00	30.00	-	-
A-TC-16C_1-1	100	120	512	612	0.0040	0.090				
A-TC-16C_1-2	099	121	511	619	0.0036	0.086				
A-TC-16C_1-3	106	122	525	621	0.0041	0.094				
Average	102±3.1^{d}	121±0.80^{e}	516±6.4^{d}	618±3.8^{e}	0.0038±0.00020^{e}	0.090±0.003^{e}	0.68	23.68	117.94	98.47

A-OTC-16C_1-1	108	131	520	668	0.0039	0.097				
A-OTC-16C_1-2	106	124	504	632	0.0038	0.092				
A-OTC-16C_1-3	112	132	509	673	0.0040	0.103				
Average	109±2.5[fg]	129±3.6[d]	511±6.7[d]	658±18.3[d]	0.0039±0.0001[d]	0.097±0.004[d]	0.74	25.00	123.45	97.52
A-NS-20M-1	157	192	550	692	0.0048	0.122				
A-NS-20M-2	161	196	510	690	0.0038	0.126				
A-NS-20M-3	168	197	539	689	0.0047	0.121				
Average	162±4.5[h]	195±2.1[hi]	533±16[h]	691±1.2[h]	0.0044±0.00045[h]	0.124±0.002[h]	1.00	28.20	-	-
A-TC-20M-1	165	192	522	670	0.0041	0.094				
A-TC-20M-2	160	186	528	650	0.0040	0.090				
A-TC-20M-3	163	189	517	663	0.0040	0.091				
Average	163±2.1[h]	189±2.4[h]	522±4.5[h]	660±8.3[i]	0.0040±0.00005[hi]	0.091±0.002[i]	0.73	22.70	123.80	97.94
A-OTC-20M-1	162	193	517	676	0.0039	0.096				
A-OTC-20M-2	167	199	533	697	0.0038	0.097				
A-OTC-20M-3	169	192	539	672	0.0037	0.100				
Average	166±2.9[h]	195±3.1[hi]	530±9.3[h]	683±11[h]	0.0038±0.00008[i]	0.097±0.002[i]	1.01	25.52	128.14	99.50
A-NS-20C_1-1	160	195	506	682	0.0046	0.126				
A-NS-20C_1-2	161	197	517	689	0.0043	0.126				
A-NS-20C_1-3	163	196	518	687	0.0047	0.132				
Average	161±1.2[j]	196±0.8[j]	514±5.4[j]	686±2.9[jl]	0.0046±0.00016[j]	0.128±0.003[j]	1.00	27.80	-	-
A-TC-20C_1-1	160	189	512	640	0.0040	0.090				
A-TC-20C_1-2	157	184	500	640	0.0036	0.086				
A-TC-20C_1-3	162	186	517	645	0.0041	0.094				
Average	160±2.1[j]	187±2.1[k]	510±7.1[j]	641±3.6[k]	0.0040±0.0002[k]	0.090±0.003[k]	0.70	22.5	124.50	99.22
A-OTC-20C_1-1	168	195	530	683	0.0040	0.096				
A-OTC-20C_1-2	166	194	528	679	0.0038	0.101				
A-OTC-20C_1-3	172	197	544	690	0.0040	0.092				
Average	169±2.5[k]	196±1.3[j]	534±7.2[k]	686±4.5[j]	0.0039±0.0001[k]	0.097±0.004[k]	1.00	25.01	133.46	103.90

***Different letters in the same column indicate significant differences ($P < 0.05$).**

**** Rebar fracture**

Table. 3. Test results of without concrete rebar tests*.

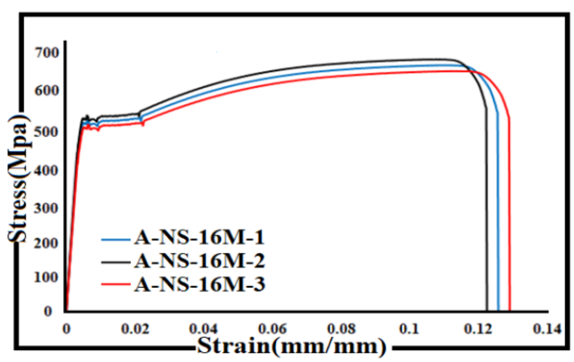

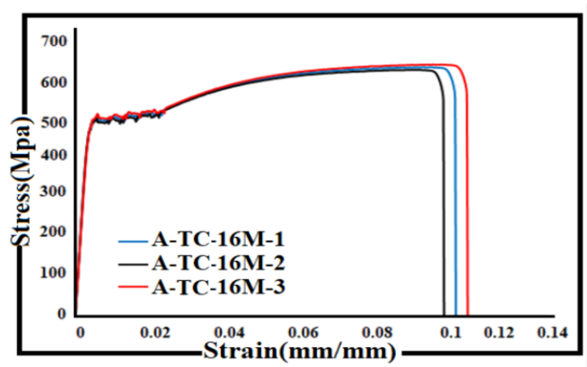

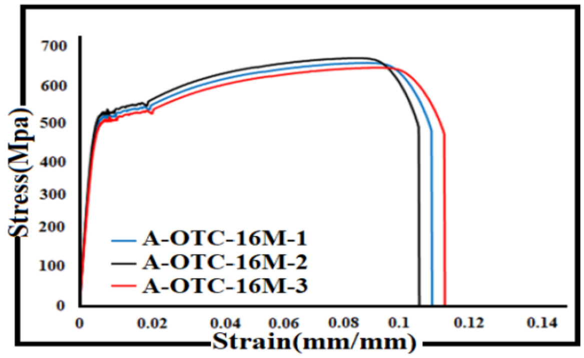
Stress(Mpa)
Strain(mm/mm)
A-OTC-16M-1
A-OTC-16M-2
A-OTC-16M-3

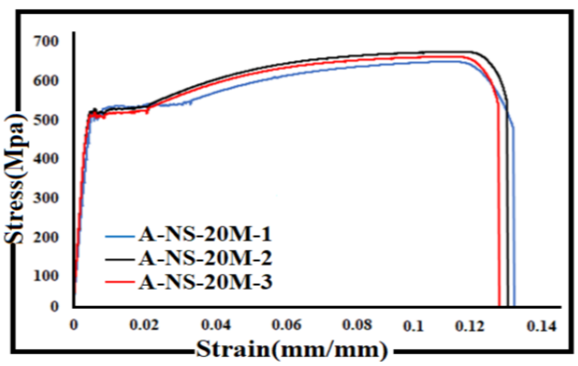
Stress(Mpa)
Strain(mm/mm)
A-NS-20M-1
A-NS-20M-2
A-NS-20M-3

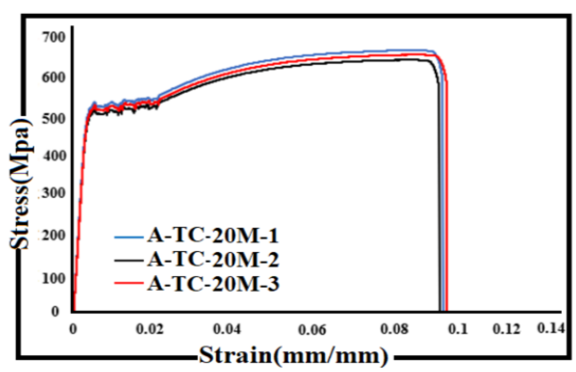
Stress(Mpa)
Strain(mm/mm)
A-TC-20M-1
A-TC-20M-2
A-TC-20M-3

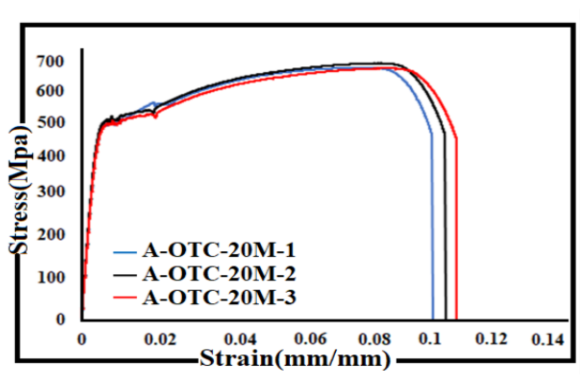
Stress(Mpa)
Strain(mm/mm)
A-OTC-20M-1
A-OTC-20M-2
A-OTC-20M-3

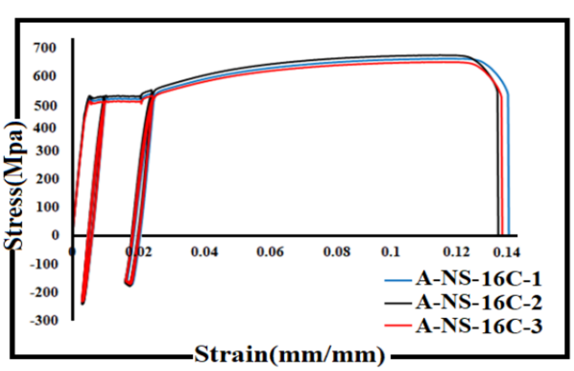
Stress(Mpa)
Strain(mm/mm)
A-NS-16C-1
A-NS-16C-2
A-NS-16C-3

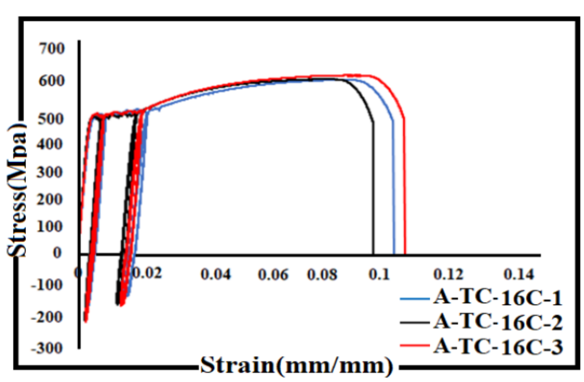
Stress(Mpa)
Strain(mm/mm)
A-TC-16C-1
A-TC-16C-2
A-TC-16C-3

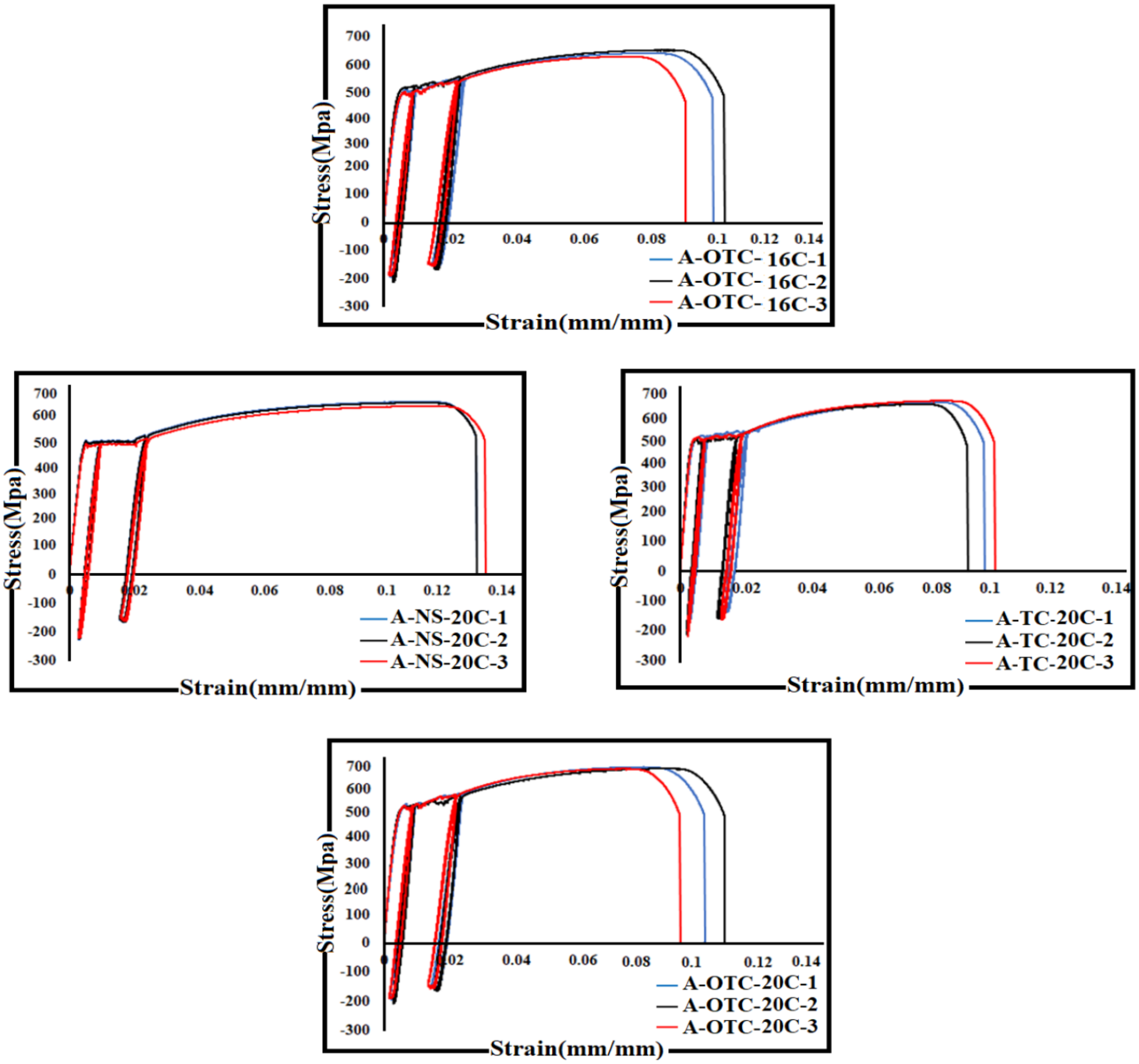

Fig. 5. Without concrete test σ-ε relationships for monotonic and cyclic specimens NS, TC and OTC (16 mm and 20 mm).

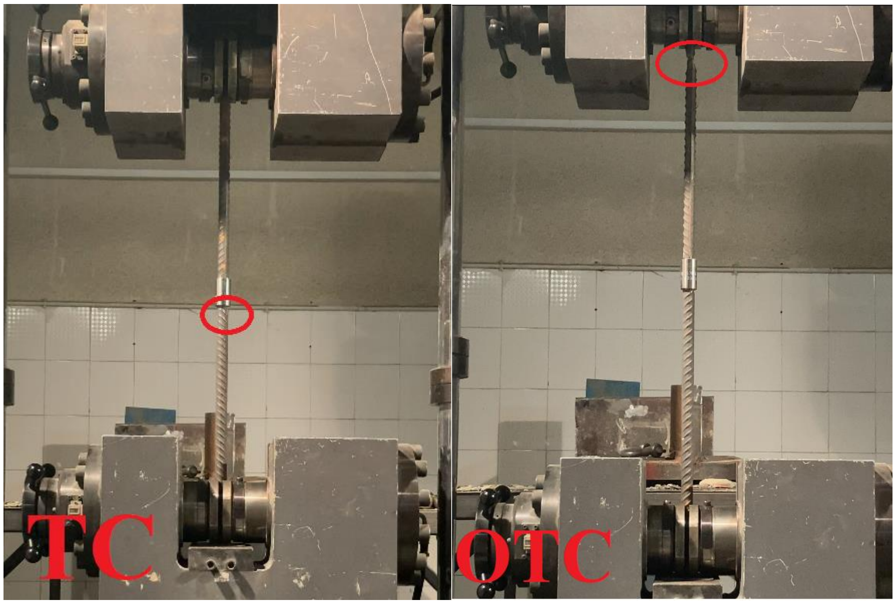

Fig. 6. Failure locations of investigated specimens NS, TC and OTC (16 mm and 20 mm):Without concrete specimens specimens.

3.3. Ductility and energy absorption

The μ and μ_ε of each sample in **Table 3** were determined using **Fig. 7** and Eq. (1) respectively.

$$Ductility\ ratio\ \ (\mu_{\varepsilon}) = \frac{ultimate\ strain\ of\ the\ splice\ bar\ (\varepsilon_{usp})}{ultimate\ strain\ \ of\ the\ non-splice\ bar(\varepsilon_{ub})} \tag{1}$$

The ultimate-to-yield mean strain ratio can be used to calculate a ductility ratio [23]. Additionally, the ratio of the ultimate strain (ε_{usp}) of the spliced bar to the ultimate strain (ε_{ub}) of the non-spliced bar can be used to assess ductility. Here, ε_{usp} stands for the ultimate strength of the spliced bar [29]. The ductility ratio ($\varepsilon_{usp}/\varepsilon_{ub}$), which is over 0.65, can satisfy the EC2 [30] and EC8 [20] requirements. When the bar class C is utilized [28], the ductility ratio ($\varepsilon_{usp}/\varepsilon_{ub}$), which is above 0.65, can satisfy the requirements of the EC2 [30] and EC8 [20] codes for medium ductility. However, the splice bar, which has a ductility ratio ($\varepsilon_{usp}/\ \varepsilon_{ub}$) less than 0.65, would seem undesirable for members that are subjected to significant inelastic deformations [29]. The above conditions should be confirmed by the splice bar's high ductility ratio, which is necessary for this investigation. According to the recommendation, the ductility of the spliced bar (μ_{sp}) should also be at least as high as that of the unspliced bar (μ_b). To employ splice bars in structural components that can bear significant seismic stresses, the ratio (μ_{sp}/μ_b) must be larger than or equal to 1.0. The ductility of the specimens was also assessed using the ($\mathcal{E}_{usp}/\mathcal{E}_{ub}$) ductility ratio recommended by the earlier study [29]. To see the outcomes According to Eq. (1), **Table 3** show the average ductility values of deformed bars (non-splice bars), splice bars, and all specimens combined. It is advised that the OTC specimen is appropriate for use in structural members with high inelastic deformation since their higher ductility value exceeds the ductility of the distorted bar, allowing them to be employed for members in seismically active areas. To withstand low-to-moderate seismic loads, TC specimens can be employed as structural elements.

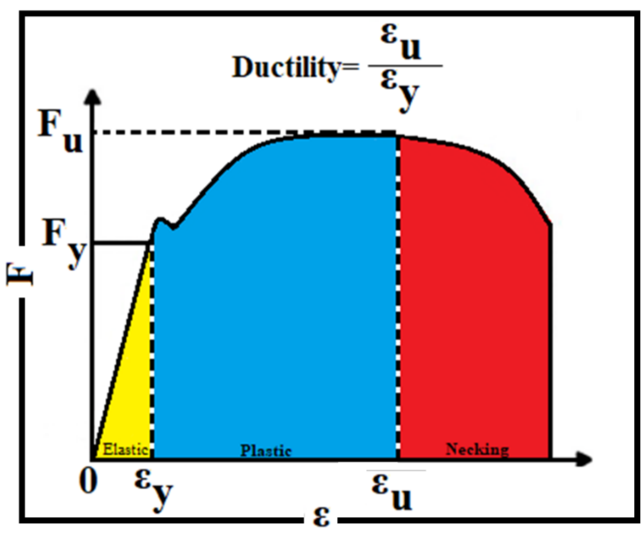

Fig. 7. yield and ultimate displacements definition[29,31]

3.4. Effect of loading mode on failure

The cyclic tension-tension loading path with a stress ratio greater than zero described in ISO 15835-1:2009 [28] is typically used in the fatigue test for the mechanical coupler failure investigation. Rebars are primarily used in RC structures to support tension stress in order to compensate for the concrete's low tensile strength. For this to be the optimal ultimate failure state of a concrete structure, the rebars in the tension zone must be destroyed at the same time that the concrete in the compression zone is damaged under compression. Therefore, only the reinforcement's tensile strength is taken into account while designing RC structures. In fact, the rebars with mechanical couplers in important RC structural components or connections are repeatedly subjected to the tension-compression load rather than the tension-tension load for RC structures under high earthquake excitation. The failure of mechanical splices under cyclic tension-compression loads, which has received less attention in the past, must obviously be studied. When the splices are exposed to compression loading, however, modest lateral displacement of the splices can be noticed, which significantly impacts the deformation of the mechanical splices under cyclic stress (**Table 3)**. As a result, even if only the strength and deformation properties of mechanical couplers are strictly inspected according to ISO 15835-1:2009 [28], they are still significantly reduced under cyclic loading, implying that mechanical splices of reinforcements in RC structures are potentially dangerous under strong earthquake excitation. To assure the safety of RC structures subjected to strong seismic excitation, it is required to evaluate the performance of mechanical splices both without concrete. Experimental research into the effects of loading mode on the failure of TC and OTC splices is presented in this paper. To ensure the safety and dependability of RC structures under the action of disasters like strong earthquakes, it is crucial to promote more in-depth experimental research based on the actual engineering situation and splicing type when novel mechanical couplers are adopted in new and important structures or in structures subjected to unusual loads.

4. Evaluation of the mechanical behavior of thread couplers

The grade of the reinforcement bars in this investigation is Grade 80 in accordance with ACI 318-19 [21]and Class C in accordance with EC8 [20]. It was discovered in thread couplers that the mechanism of the threaded bar and coupler on the bar had adequate interlocking strength to prevent slip displacement. The embedded thread diameter, on the other hand, is critical in ensuring the high performance of threaded couplers. Due to the high engagement strength of the strong connector in the threaded section, no slip displacement in the side of the threaded bar was detected. To observe stronger bonding between the thread and couplers, the thread position's cross-section area should be larger. In the event of a larger cross-sectional area of the bar, the bonding stresses will be uniform on the bar surface. ACI 318-19 [17], ACI 439 [32], and AC-133 [33], as well as the ISO 15835-Part 1: 2018 and ISO 15835-Part 2: 2018 standards [28], all indicate the recommended conditions for a mechanical splice utilizing a coupler. The ultimate tensile strength of the mechanical splice should be greater than 1.25 times the bar yield strength, according to BS-8110 [34] and ACI 318-19 [17] specifications. Thus, it is crucial to assess each sample's ultimate strength ratio (R_u). In this study, R_u stands for the ratio of the thread coupler sample's ultimate tensile strength to the average yield tensile strengths of the specimens of deformed bar (non-splice bar). In the case of OTC couplers, they satisfy ACI 318 specifications (**Table 3**). Unfortunately, some bars do not have the potential to be oversize, or, in other words, after the rebar is oversized, the hardness of the threading area increases significantly, making threading problematic. There is no forming process. Furthermore, the yield strength ratio (R_y) was calculated; R_y signifies the ratio of the thread coupler sample's yield tensile strength to the average yield tensile strength of the deformed bars (**Table 3**). While the average Ry ratios in OTC and TC are less than 1.0, In comparison to other couplers, OTC couplers perform best in terms of strengths (Ru and Ry), ductility, energy dissipation, and failure mode. Due to their improved performance, the equal splicing of RFWTC and OTC samples makes them ideal for use in high seismic zones. Additionally, the TC's performances in terms of strength, energy dissipation, and failure mode have met the standards. The structural part can withstand low-to-medium earthquake loads thanks to the ductility value of Therefore.

5.Conclusions

In this study, by modifying the method of making a threaded splice, one type of patch is introduced that can be used in the plastic hinge areas of ductile members in seismic areas. The splice area in the suggested method is oversized. In this study, more than 36 threaded couplers and oversize-threaded couplers were tested under uniaxial tensile and cyclic conditions on NC, TC, and OTC reinforcement bars with diameters of 16 mm and 20 mm. Specimens to determine the influence of the threaded diameter on strength, ductility, and energy absorption. The following judgments were reached:

1. In the elastic cycle test, the OTC coupler exhibited somewhat equal stresses to the non-spliced reference bar, with no noticeable slide at the threads. Cyclic loading also had a negative influence on the without-concrete response, with strain at fracture reductions of up to 18% on average when compared to monotonic examples. The detailed strain measurements revealed that the enlarged rebar cross-section near the threads of couplers shifts the weak area away from the coupler region.
2. The behavior of the OTC meets the good performance requirements for the structural member subjected to the cyclic loading test and meets the seismic zone standards. Due to its improved

performance, the equal splicing of the OTC sample makes it ideal for use in high seismic zones. Additionally, the TC's performances in terms of strength, energy dissipation, and failure mode have met the standards. The structural part can withstand low-to-medium earthquake loads thanks to the ductility value of Therefore.

3. One key factor that may be utilized to assess the behavior of couplers is their energy absorption. For increased energy absorption compared to a non-splice bar, the OTC requires the threading size be increased by one size. The ultimate tensile load capacity of the couplers will increase with an increase in the thread area. The embedded bar length in the OTC shows the best performance. The OTC's ductility ratio was higher than the non-splice bar. According to practical design codes, the strength of the OTC specimens is greater than 125% of the bar yield strength.

4. The yield and ultimate strengths of OTC are comparable to those of NC, and they can also fulfill the strength requirement in the alternating tension and compression test with high stresses. Considering the outstanding connection efficiency and ease of OTC, the mechanical connection of rebars has substantially higher benefits.

Acknowledgements

The authors would like to thank the logistical support provided by the IIEES (International Institute of Earthquake Engineering and Seismology in Tehran, Iran).

Nomenclature

A_c	Cross-sectional concrete
A_{co}	Cross-sectional area
D	Coupler Diameter
D_1	Concrete Diameter
E_{tc}	Elastic modulus of the coupler
F	Load
F_c	Load of the concrete
F_y	Yield load
Fu	Ultimate load/peak load
F_{us}	Thread splice sample's load-carrying capacity
F_{ut}	Ultimate tensile load of the threaded area in the bar and coupler
F_{uc}	Tensile load resistance of the concrete
K	Stress concentration factor
L	Specimen length
L_{Con}	Concrete Length
L_C	Coupler length
L_S	Splice length
L_T	Thread Length

٣٤٧	L_W	Welding Length
٣٤٨	R_y	Yield strength ratio
٣٤٩	R_u	Ultimate strength ratio
٣٥٠	ε_{tc}	Strain in the coupler
٣٥١	ε_{c0}	Concrete strain at peak stress
٣٥٢	ε_{cu}	Concrete ultimate strain
٣٥٣	ε_{usp}	Ultimate strain of the splice bar
٣٥٤	ε_{ub}	Ultimate strain of the non-splice bar
٣٥٥	ε_{co}	Strain of the coupler
٣٥٦	ε_{c0}	Concrete strain at peak stress
٣٥٧	ε_{cu}	Concrete ultimate strain
٣٥٨	ε_{f}	Failure strain of steel bars
٣٥٩	ε_{y}	Yield strain of steel bars
٣٦٠	ε_{u}	Ultimate strain of steel bars
٣٦١	σ_{tc}	Stress of the coupler
٣٦٢	σ_{co}	Determine the coupler's design transverse tensile stress
٣٦٣	σ_{max}	Maximum stress
٣٦٤	σ_{nom}	Nominal stress

f_u Ultimate strength

μ Ductility

μ_ε Ductility ratio

β Coefficient based on the bar type

d_b Steel bar Diameter

d_1 Thread area

d_2 Bar oversize

d_3 Thread pitch

f'_c Equivalent compressive strength of cylinder sample

f_{cr} Compressive concrete strength

f_y Yield strength

Reference

[1] Nateghi-Alahi F, Shokrzadeh MR. Behavior considerations for mechanical rebar couplers. Behavior considerations for mechanical rebar couplers, University of Tokyo: 2019, p. 30–41.

[2] Shokrzadeh MR, Nateghi Allahe F, Mansoori , Mohammad Reza, Javadi P, Mansoori, MR, Javadi P. Failure area evaluation of the coupler with threaded bar: Experimental and Numerical study. International Journal of Advanced Structural Engineering 2022;12:531–

43. https://doi.org/10.1007/IJASE.2022.692294.

[3] Shokrzadeh MR, Nateghi-Alahi F, Mansoori MR, Javadi P. The improvement of the threaded-based mechanical splice by modifying the threaded system: Study of techniques cold rolling and rotating friction welding. Journal of Building Engineering 2023;80:107964. https://doi.org/10.1016/J.JOBE.2023.107964.

[4] Tazarv M, Shrestha G, Saiidi MS. State-of-the-art review and design of grouted duct connections for precast bridge columns. Structures 2021. https://doi.org/10.1016/j.istruc.2020.12.091.

[5] Shokrzadeh MR. Experimental study of seismic behavior and modification of the failure region of mechanical bar splices in reinforced concrete vertical elements. Islamic Azad University Science and Research Branch, 2024.

[6] Einea A, Yehia S, Tadros MK. Lap splices in confined concrete. ACI Structural Journal 1999;96:947–55. https://doi.org/10.14359/769.

[7] Lee CS, Han SW. Cyclic behaviour of lightly-reinforced concrete columns with short lap splices subjected to unidirectional and bidirectional loadings. Engineering Structures 2019. https://doi.org/10.1016/j.engstruct.2019.03.108.

[8] Kheyroddin A, Dabiri H. Cyclic performance of RC beam-column joints with mechanical or forging (GPW) splices; an experimental study. Structures 2020. https://doi.org/10.1016/j.istruc.2020.10.071.

[9] Dabiri H, Kheyroddin A. An experimental comparison of RC beam-column joints incorporating different splice methods in the beam. Structures 2021.

https://doi.org/10.1016/j.istruc.2021.08.101.

[10] Yamamoto RI, Fukada Y, Tatsumi M, Ueyama K. New quality inspection method for gas pressure welds. Quarterly Report of RTRI (Railway Technical Research Institute) (Japan) 2002. https://doi.org/10.2219/rtriqr.43.7.

[11] Rodrigues H, Furtado A, Arêde A, Vila-Pouca N, Varum H. Experimental study of repaired RC columns subjected to uniaxial and biaxial horizontal loading and variable axial load with longitudinal reinforcement welded steel bars solutions. Engineering Structures 2018. https://doi.org/10.1016/j.engstruct.2017.11.043.

[12] Sharbatdar MK, Jafaria OM, Karimib MS. Experimental evaluation of splicing of longitudinal bars with forging welding in flexural reinforced concrete beams. Advances in Concrete Construction 2018. https://doi.org/10.12989/acc.2018.6.5.509.

[13] Dabiri H, Kheyroddin A, Faramarzi A. Predicting tensile strength of spliced and non-spliced steel bars using machine learning- and regression-based methods. Construction and Building Materials 2022. https://doi.org/10.1016/j.conbuildmat.2022.126835.

[14] Dahal PK, Tazarv M. Mechanical bar splices for incorporation in plastic hinge regions of RC members. Construction and Building Materials 2020;258:120308. https://doi.org/10.1016/j.conbuildmat.2020.120308.

[15] Bompa D V., Elghazouli AY. Inelastic cyclic behaviour of RC members incorporating threaded reinforcement couplers. Engineering Structures 2019;180:468–83. https://doi.org/10.1016/j.engstruct.2018.11.053.

[16] Wu S, Li H, Wang X, Li R, Tian C, Hou Q. Seismic performance of a novel partial precast

RC shear wall with reserved cast-in-place base and wall edges. Soil Dynamics and Earthquake Engineering 2022. https://doi.org/10.1016/j.soildyn.2021.107038.

[17] ACI 318-19 Building Code Requirements for Structural Concrete and Commentary. 318-19 Building Code Requirements for Structural Concrete and Commentary 2019. https://doi.org/10.14359/51716937.

[18] Caltrans. Caltrans Seismic Design Criteria Version 1.7. California Department of Transportation: Sacramento, CA, US 2013.

[19] AASHTO. AASHTO LRFD Bridge Design Specifications, 9th Edition. 2020.

[20] European Commitee for Standardization. Eurocode 8: Design of structures for earthquake resistance - Part 1 : General rules, seismic actions and rules for buildings. European Committee for Standardization 2004.

[21] ACI Committee 318. Aci 318 - 19 Building Code Requirements for Structural Concrete and Commentary. 2019.

[22] Zhao E, Song C, Zhang X, Zhou Q, Yan K. Experimental study on monotonic, cyclic mechanics and fatigue performance of pressed cone sleeve splices. Structures 2022. https://doi.org/10.1016/j.istruc.2022.03.050.

[23] Bompa D V., Elghazouli AY. Monotonic and cyclic performance of threaded reinforcement splices. Structures 2018;16:358–72. https://doi.org/10.1016/j.istruc.2018.11.009.

[24] Al-Jelawy HM. Experimental and numerical investigations on monotonic tensile behavior of grouted sleeve couplers with different splicing configurations. Engineering Structures

2022;265:114434. https://doi.org/10.1016/J.ENGSTRUCT.2022.114434.

[25] Liu C, Pan L, Liu H, Tong H, Yang Y, Chen W. Experimental and numerical investigation on mechanical properties of grouted-sleeve splices. Construction and Building Materials 2020. https://doi.org/10.1016/j.conbuildmat.2020.120441.

[26] Tazarv M, Saiidi MS. Seismic design of bridge columns incorporating mechanical bar splices in plastic hinge regions. Engineering Structures 2016. https://doi.org/10.1016/j.engstruct.2016.06.041.

[27] ASTM Standard E8/E8M. Standard Test Methods for Tension Testing of Metallic Materials, ASTM International, West Conshohocken, PA, 2011. ASTM International 2016.

[28] ISO/DIS 15835. Steel for the Reinforcement of Concrete - Reinforcement Couplers for Mechanical Splices of Bars (Parts 1 to 3). International Organizationa for Standardization, Geneva, Switzerland; 2018. n.d.

[29] Bompa D V., Elghazouli AY. Ductility considerations for mechanical reinforcement couplers. Structures 2017. https://doi.org/10.1016/j.istruc.2017.08.007.

[30] British Standards I. Eurocode2: Design of Concrete Structures: Part 1-1: General Rules and Rules for Buildings. British Standards Institution 2004.

[31] Shokrzadeh MR, Nateghi-Alahi F. Evaluation of hybrid NSM-CFRP technical bars and FRP sheets for seismic rehabilitation of a concrete bridge pier. Bridge Structures 2022;18:75–88. https://doi.org/10.3233/BRS-290180.

[32] ACI Committee 439. Types of mechanical splices for reinforcing bars. 2007.

[33] AC133 - ICC Evaluation Service, LLC (ICC-ES) n.d. https://icc-es.org/acceptance-criteria/ac133/ (accessed December 13, 2022).

[34] Kirkbridge TW. Structural use of concrete — Part 1: Code of practice for design and construction. 1997.